Proceedings of the Canadian Society for Mechanical Engineering International Congress
32nd Annual Conference of the Computational Fluid Dynamics Society of Canada
Canadian Society of Rheology Symposium
CSME-CFDSC-CSR 2025
May 25–28, 2025, Montréal, Québec, Canada

Laser Powder Bed Fusion Optimal Process Window for Tensile Strength of Ti-6AL-4V

Thanh-Liem Huynh[1], Shubham Chaudhry[1], David Holsworth[1], Viet-Hung Vu[1]
[1]Department of Mechanical and Aerospace Engineering, Royal Military College, Kingston, Canada

Abstract—This paper investigates the tensile strength of Ti-6Al-4V produced by laser powder bed fusion, focusing on the development of an optimal process window and the prediction of tensile strength. A drastic literature review enables the construction of the optimal process window for the laser powder bed fusion of Ti-6Al-4V. The process window is then fine-tuned for the tensile strength, especially with the OneClick Metal machine. Within this process window, tensile strength can be predicted from the literature and validated through the experimental testing of the tensile strength properties of the OneClick Metal machine.

Keywords-component—Laser Powder Bed Fusion, Tensile Strength, Process Window.

I. INTRODUCTION

Laser powder bed fusion (L-PBF) is one of the most widely used additive manufacturing (AM) technologies in powder bed fusion (PBF). L-PBF forms parts by adding material layer-by-layer based on computer design data, with each layer created by melting separate passes of powder material that is rapidly heated, melted, solidified, and cooled during deposition [1]. The advantages of the process include exceptional resolution due to the ability to focus the laser beam to a precise spot size on the powder bed [2]. This leads to a small melt pool, which results in a better surface quality of the manufactured part. Overall, the L-PBF process is characterized by its precise resolution and excellent surface quality, making it a preferred choice for the production of intricate and high-quality components [3].

Ti-6Al-4V accounts for about 50% of total titanium production and is a popular choice in the biomedical and aerospace industries due to its high biocompatibility and strength [4]. Since the 1960s, Ti-6Al-4V has been used as a structural material in modern airplanes. In the aerospace industry, it is mainly used for engine parts and airframes, including components such as seat rails and bolts. Due to its relatively low allowable working temperature of around 300 °C, Ti-6Al-4V is often used for fans, fan cases, blades, and other engine parts that operate below this temperature [5]. The exceptional mechanical performance of Ti-6Al-4V results from its vanadium and aluminum alloying elements, which allow the microstructure to retain both the α and β phases at room temperature.

L-PBF process parameters of particular importance are laser power (P-Watt); scanning speed (v–mm/s); hatch spacing (h-μm); and layer thickness (t-μm). These four parameters must be taken into account in the process window as they all influence the total energy (E-J/mm^3) that the laser transfers to the powder bed. They have a direct effect on how the layer is built up and usually need to be adjusted to optimize the density [6,7,8]. The formula for energy density is as follows

$$E = \frac{P}{v.h.t}$$

Industrial applications depend on the mechanical properties of materials produced from Ti-6Al-4V by laser powder bed fusion, especially tensile strength, microhardness, and fatigue strength, and the understanding the effects of process parameters on these properties is of great significance. In particular, this paper specifically reviews the relationship between the tensile properties of L-PBF Ti-6Al-4V and the process parameters (laser power, scanning speed, hatch spacing, and layer thickness), predicts the optimal process window to achieve optimal tensile strength of Ti-6Al-4V, and validates the predicted results by experiments.

II. REVIEW OF LITERATURE

A. Effect of energy density on the tensile properties of additive-manufactured Ti-6Al-4V

Numerous researchers have investigated how process parameters—particularly energy density—affect the tensile properties of as-built Ti-6Al-4V produced by laser powder bed fusion (L-PBF) and selective laser melting (SLM), including Aung Nyein Soe et. al. [18]; N. Baskin & C. Yuce [16]; Snehashis Pal et. al. [14]; Xi Du et. al. [15]; J. Ju et. al. [13]; Jiangwei Liu et. al. [24]; X. Yan et. al. [21]; P. Edwards et. al. [22]; Bey Vrancken et. al. [19]; T. Vilaro et. al. [10]; B. Vandenbroucke and J.-P. Kruth [26], etc... They found that AM Ti-6Al-4V samples typically exhibits high tensile strength

(1100–1400 MPa) but low ductility (<10%). For example, Aung Nyein Soe et al. [18] achieved an average ultimate tensile strength (UTS) of 1193 MPa, yield strength (YS) of 992.6 MPa, and elongation at break (EL) of 4.8% using an energy density of 83 J/mm³. Snehashis Pal et al [14] reported UTS of 1437 MPa, YS of 1250 MPa, and EL of 5.6% with energy density of 65 J/mm³. (See Table 1 and Fig. 1)

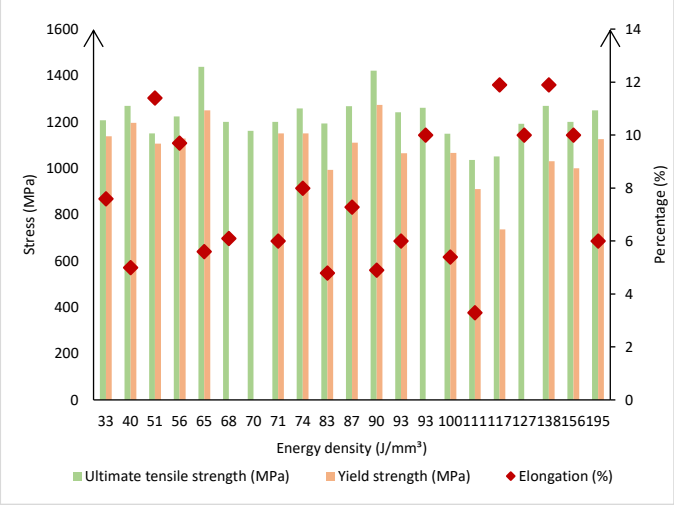

Figure 1. Effect of energy density on the tensile properties of PBF Ti-6Al-4V

B. *Effect of laser power on tensile properties of additive-manufactured Ti-6Al-4V*

Niyazi Baskin and Celalettin Yuce et al. [16] and Amit Kumar Singh Chauhan et al. [27] found an improved tensile strength with increased laser power. However, in the study by J. Liu et al. [14], Fan Zhechao et. al. [28], and F.R. Kaschel et. al. [29], opposite results were observed. They found that an increase in laser power initially improved the tensile strength up to a certain point, after which further increases led to a decrease in both tensile strength and elongation. (See Table 2 and Fig. 2)

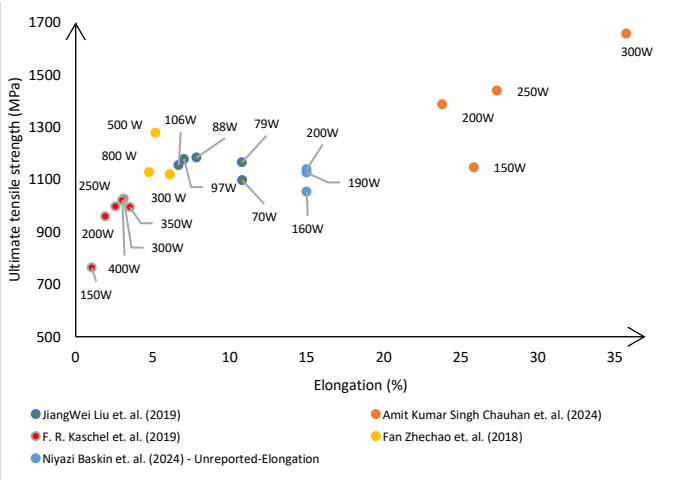

Figure 2. Effect of laser power on the tensile properties of Ti-6Al-4V

C. *Effect of scanning speed on tensile properties of additive-manufactured Ti-6Al-4V*

Niyazi Baskin and Celalettin Yuce et al [16] and Amit Kumar Singh Chauhan et al. [27] found an improved tensile strength with increased laser power. However, in the study by J. Liu et al [24], Fan Zhechao et al [28], and F.R. Kaschel et al. [29], opposite results were observed. They found that an increase in laser power initially improved the tensile strength up to a certain point, after which further increases led to a decrease in both tensile strength and elongation. (See Table 3 and Fig. 3)

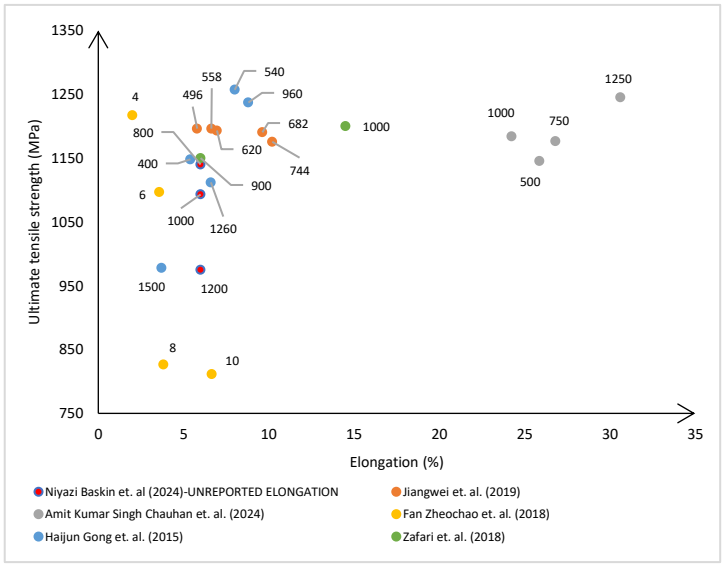

Figure 3. Effect of scanning speed on the tensile properties of Ti-6Al-4V

D. *Effect of hatch spacing on tensile properties of additive-manufactured Ti-6Al-4V*

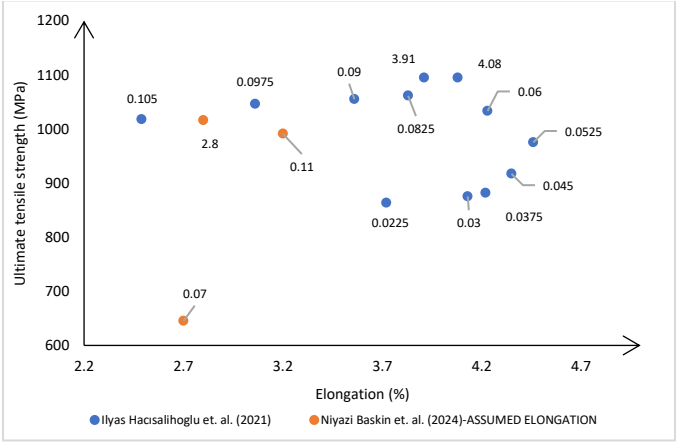

Figure 4. Effect of hatch spacing on the tensile properties of Ti-6Al-4V

Niyazi Baskin, Celalettin Yuce et al. [16] and Ilyas Hacısaliho˘glu et al. [30] explored the tensile properties with varied hatch spacing and stated that the ultimate tensile strength increases with increasing hatch spacing and also found that hatch spacing within 0.06 mm to 0.1 mm exhibited the relatively

unchanged ultimate tensile strength and elongation (See Table 4 and Fig. 4). Upon reviewing the literature, the optimal hatch spacing to achieve the desired mechanical properties is between 61–100 µm, as reported by T. Vilaro et al. [10]. These findings are consistent with the study of Galina Kasperovich et al. [8] that suggests a scan range of less than 60 µm is not recommended, as it leads to significant pore generation in the peripheral regions of L-PBF samples. Effect of layer thickness on tensile properties of additive-manufactured Ti-6Al-4V

The layer thickness in research studies on Ti-6Al-4V varies depending on the powder size and the process parameters, but the tensile properties of Ti-6Al-4V remain constant with slight changes (See Table 5 and Fig. 5). A layer thickness of 20-30 µm is commonly used for the production of Ti-6Al-4V to ensure part quality.

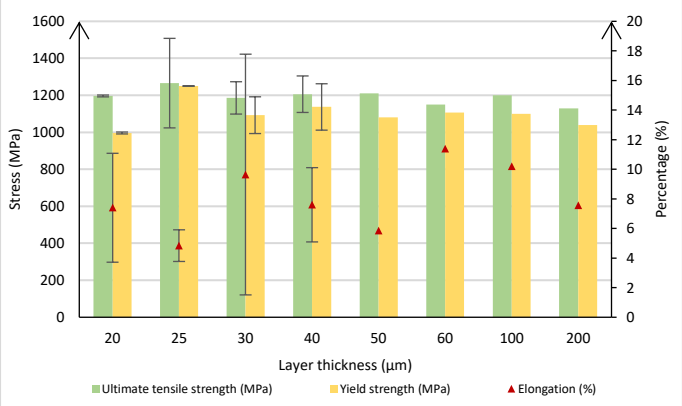

Figure 5. Effect of layer thickness on the tensile properties of Ti-6Al-4V

III. Optimal process window for tensile strength

A few authors have developed process windows for SLM-Ti-6Al-4V samples based on the correlation between energy density, varying laser powers, and scanning speeds with porosity. Gong et al. [6] predicted the limit of the working range of SLM Ti-6Al-4V with the energy density between 74 and 100 J/mm³ and found the porosity to be 1 and 5 %, respectively and the tensile properties to be UTS of 1148 – 1257 MPa, YS of 1066 – 1150 MPa and EL of 10.9 – 11.1 %. Han et al. [7] found that the densities ranged from 99.82 to 99.98 %, with an energy density of 80 J/mm³ to 190 J/mm³, and the tensile properties at 138 J/mm³ showed UTS of 1268 MPa, YS of 1030 MPa, and EL of 11.9 %. The limit of energy densities between 58 and 146 J/mm³ by Galina Kasperovich et al [8]. showed a porosity of less than 5% and the tensile properties at 117 J/mm³ minimum porosity, a UTS of 1051 MPa, YS of 736 MPa, and EL of 11.9 %. Patcharapit Promoppatum et al. [32] have mapped the process window in which continuous melting can be achieved when working with an energy density of more than 36.9 J/mm³ but less than 87 J/mm³, while the scanning speed remains higher. Therefore, the boundary of operating to produce the Ti-6Al-4V parts with optimal tensile properties could be between 36.9 J/mm³ and 146 J/mm³. The energy density data points with varying laser powers and scanning speeds that are plotted based on Table 1 and the boundary of the operating region (in blue cuboid) are shown in Figure 6.

The collected data points of the relationship between the optimal process parameters and the tensile properties of Ti-6Al-4V in Table 1; the regions (1-Green zone, 2-Gray zone, 3-Orange zone) in the process windows that produce a high-quality part with minimal porosity, which were developed by Patcharapit Promoppatum et. al. [32], Gong et. al. [6,9], Song et. al. [33]; as well as the operational capability of the MPrint – One Click Metal machine (200W fiber laser and up to 3000 mm/s scanning speed) allow the comprehensive process window for One Click Metal machine to be mapped in the blue zones of the following Figure 7.

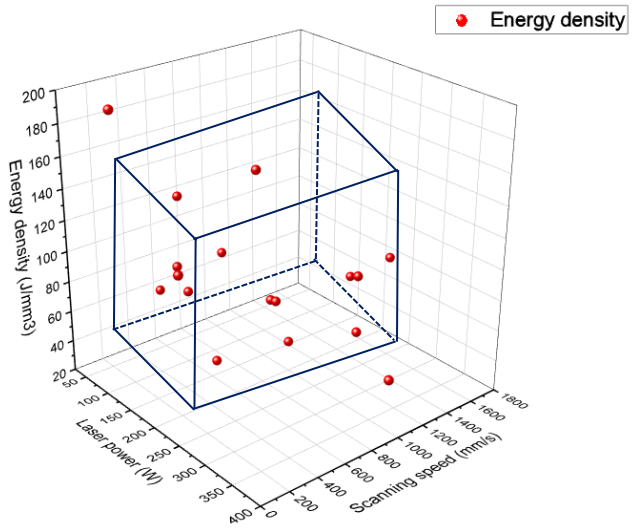

Figure 6. The boundary of operating region at energy densities of Ti-6Al-4V

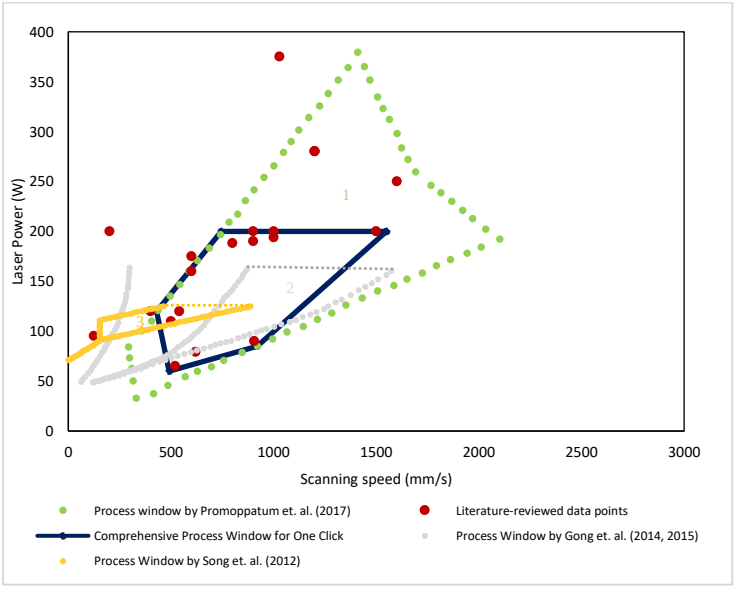

Figure 7. An assessment of the relationship between scanning speed and laser power as reported in the literature. The data points discovered in the literature is compared to the process windows as reported Patcharapit Promoppatum et al. [32], Gong et al. [6,9], Song et al. [33]

IV. CONCLUSION

The comprehensive process window for L-PBF Ti-6Al-4V in Figure 7 represents the range of laser power and scanning speed. The limits of laser power are between 60 and 200 W, and the scanning speed ranges from 400 to 1600 mm/s. Within this window and the boundary of operating region in Figure 5, the energy densities are between 36.9 J/mm^3 to 146 J/mm^3. The predicted tensile properties from the literature for Ti-6Al-4V within the optimal process window are: UTS (1051 – 1437 MPa), YS (736 – 1250 MPa), and EL (4.8 – 11.9 %).

Our next research will be to experimentally print the specimens and conduct tensile tests to compare the experimental results with the predicted tensile strength from the literature within the process window. This approach will help to refine the process parameters and improve the reliability and performance of L-PBF Ti-6Al-4V components in industrial applications.

ACKNOWLEDGMENT

The authors acknowledge support from the DIRECTOR GENERAL AEROSPACE EQUIPMENT PROGRAM MANAGEMENT DIVISION via the Aerospace Engineering Technical Investigations and Academic Services program

REFERENCES

[1] E. Uhlmann, R. Kersting, T. B. Klein, M. F. Cruz, and A. V. Borille, "Additive Manufacturing of Titanium Alloy for Aircraft Components," in Procedia CIRP, Elsevier B.V., 2015, pp. 55–60. doi: 10.1016/j.procir.2015.08.061.

[2] M. Ghayoor, K. Lee, Y. He, C.-H. Chang, B. K. Paul, and S. Pasebani, "Selective Laser Melting of 304L Stainless Steel: Role of Volumetric Energy Density on the 1 Microstructure, Texture and Mechanical Properties 2," 2019. [Online]. Available: https://www.elsevier.com/open-access/userlicense/1.0/

[3] H. K. Rafi, N. V. Karthik, H. Gong, T. L. Starr, and B. E. Stucker, "Microstructures and mechanical properties of Ti6Al4V parts fabricated by selective laser melting and electron beam melting," J Mater Eng Perform, vol. 22, no. 12, pp. 3872–3883, Dec. 2013, doi: 10.1007/s11665-013-0658-0.

[4] Rahul, D. K. Mishra, S. Datta, and M. Masanta, "Effects of Tool Electrode on EDM Performance of Ti-6Al-4V," Silicon, vol. 10, no. 5, pp. 2263–2277, Sep. 2018, doi: 10.1007/s12633-018-9760-0.

[5] I. Inagaki, T. Takechi, Y. Shirai, and N. Ariyasu, "Application and features of titanium for the aerospace industry," Nippon Steel & Sumitomo Metal Technical Report, vol. 106, no. 106, pp. 22–27, 2014.

[6] H. Gong, K. Rafi, H. Gu, G. D. Janaki Ram, T. Starr, and B. Stucker, "Influence of defects on mechanical properties of Ti-6Al-4V components produced by selective laser melting and electron beam melting," Mater Des, vol. 86, pp. 545–554, Dec. 2015, doi: 10.1016/j.matdes.2015.07.147

[7] J. Han et al., "Microstructure and mechanical property of selective laser melted Ti6Al4V dependence on laser energy density," Rapid Prototyp J, vol. 23, no. 2, pp. 217–226, 2017, doi: 10.1108/RPJ-12-2015-0193.

[8] G. Kasperovich, J. Haubrich, J. Gussone, and G. Requena, "Correlation between porosity and processing parameters in TiAl6V4 produced by selective laser melting," Mater Des, vol. 105, pp. 160–170, Sep. 2016, doi: 10.1016/j.matdes.2016.05.070.

[9] Gong, H., Rafi, K., Gu, H., Starr, T., & Stucker, B., "Analysis of defect generation in Ti-6Al-4V parts made using powder bed fusion additive manufacturing processes", Additive Manufacturing, 1, 87–98, 2014. doi: 10.1016/j.addma.2014.08.002

[10] T. Vilaro, C. Colin, and J. D. Bartout, "As-fabricated and heat-treated microstructures of the Ti-6Al-4V alloy processed by selective laser melting," Metall Mater Trans A Phys Metall Mater Sci, vol. 42, no. 10, pp. 3190–3199, Oct. 2011, doi: 10.1007/s11661-011-0731-y.

[11] Zhao, X., Li, S., Zhang, M., Liu, Y., Sercombe, T. B., Wang, S., Hao, Y., Yang, R., & Murr, L. E. (2016). Comparison of the microstructures and mechanical properties of Ti-6Al-4V fabricated by selective laser melting and electron beam melting. Materials and Design, 95, 21–31. https://doi.org/10.1016/j.matdes.2015.12.135

[12] Leuders, S., Thöne, M., Riemer, A., Niendorf, T., Tröster, T., Richard, H. A., & Maier, H. J. (2013). On the mechanical behaviour of titanium alloy TiAl6V4 manufactured by selective laser melting: Fatigue resistance and crack growth performance. International Journal of Fatigue, 48, 300–307. https://doi.org/10.1016/j.ijfatigue.2012.11.011

[13] J. Ju, J. Li, C. Yang, K. Wang, M. Kang, and J. Wang, "Evolution of the microstructure and optimization of the tensile properties of the Ti–6Al–4V alloy by selective laser melting and heat treatment," Materials Science and Engineering: A, vol. 802, Jan. 2021, doi: 10.1016/j.msea.2020.140673

[14] S. Pal et al., "Fine martensite and beta-grain variational effects on mechanical properties of Ti–6Al–4V while laser parameters change in laser powder bed fusion," Materials Science and Engineering: A, vol. 892, Feb. 2024, doi: 10.1016/j.msea.2023.146052

[15] X. Du, M. Simonelli, J. W. Murray, and A. T. Clare, "Facile manipulation of mechanical properties of Ti-6Al-4V through composition tailoring in laser powder bed fusion," J Alloys Compd, vol. 941, Apr. 2023, doi: 10.1016/j.jallcom.2023.169022

[16] N. Baskin and C. Yuce, "Effect of process parameters on the mechanical behavior of Ti6Al4V alloys fabricated by laser powder bed fusion method," Journal of Materials Research and Technology, vol. 30, pp. 7006–7019, May 2024, doi: 10.1016/j.jmrt.2024.05.084

[17] Hartunian, P., & Eshraghi, M. (2018). Effect of build orientation on the microstructure and mechanical properties of selective laser-melted Ti-6Al-4V Alloy. Journal of Manufacturing and Materials Processing, 2(4). https://doi.org/10.3390/jmmp2040069

[18] Soe, A. N., Sombatmai, A., Promoppatum, P., Srimaneepong, V., Trachoo, V., & Pandee, P. (2024). Effect of post-processing treatments on surface roughness and mechanical properties of laser powder bed fusion of Ti–6Al–4V. Journal of Materials Research and Technology, 32, 3788–3803. https://doi.org/10.1016/j.jmrt.2024.08.197

[19] B. Vrancken, L. Thijs, J. P. Kruth, and J. Van Humbeeck, "Heat treatment of Ti6Al4V produced by Selective Laser Melting: Microstructure and mechanical properties," J Alloys Compd, vol. 541, pp. 177–185, Nov. 2012, doi: 10.1016/j.jallcom.2012.07.022

[20] B. Wysocki, P. Maj, R. Sitek, J. Buhagiar, K. J. Kurzydłowski, and W. Świeszkowski, "Laser and electron beam additive manufacturing methods of fabricating titanium bone implants," *Applied Sciences (Switzerland)*, vol. 7, no. 7, Jun. 2017, doi: 10.3390/app7070657.

[21] X. Yan et al., "Effect of heat treatment on the phase transformation and mechanical properties of Ti6Al4V fabricated by selective laser melting," J Alloys Compd, vol. 764, pp. 1056–1071, Oct. 2018, doi: 10.1016/j.jallcom.2018.06.076

[22] P. Edwards and M. Ramulu, "Fatigue performance evaluation of selective laser melted Ti-6Al-4V," Materials Science and Engineering: A, vol. 598, pp. 327–337, Mar. 2014, doi: 10.1016/j.msea.2014.01.041

[23] G. Kasperovich and J. Hausmann, "Improvement of fatigue resistance and ductility of TiAl6V4 processed by selective laser melting," J Mater Process Technol, vol. 220, pp. 202–214, 2015, doi: 10.1016/j.jmatprotec.2015.01.025

[24] J. Liu et al., "Achieving Ti6Al4V alloys with both high strength and ductility via selective laser melting," Materials Science and Engineering: A, vol. 766, Oct. 2019, doi: 10.1016/j.msea.2019.138319

[25] C. Qiu, N. J. E. Adkins, and M. M. Attallah, "Microstructure and tensile properties of selectively laser-melted and of HIPed laser-melted Ti-6Al-4V," Materials Science and Engineering: A, vol. 578, pp. 230–239, Aug. 2013, doi: 10.1016/j.msea.2013.04.099

[26] B. Vandenbroucke and J.-P. Kruth, "Selective laser melting of biocompatible metals for rapid manufacturing of medical parts".

[27] A. K. S. Chauhan, M. Shukla, and A. Kumar, “Effect of Laser Sintering Parameters on the Microstructure, Mechanical Properties and Corrosion Behavior of Titanium Grade 5 Alloy,” J Mater Eng Perform, Nov. 2024, doi: 10.1007/s11665-024-09935-0

[28] Z. Fan and H. Feng, “Study on selective laser melting and heat treatment of Ti-6Al-4V alloy,” Results Phys, vol. 10, pp. 660–664, Sep. 2018, doi: 10.1016/j.rinp.2018.07.008

[29] F. R. Kaschel, M. Celikin, and D. P. Dowling, “Effects of laser power on geometry, microstructure and mechanical properties of printed Ti-6Al-4V parts,” J Mater Process Technol, vol. 278, Apr. 2020, doi: 10.1016/j.jmatprotec.2019.116539

[30] I. Hacısalihoğlu, F. Yıldiz, and A. Çelik, “The effects of build orientation and hatch spacing on mechanical properties of medical Ti–6Al–4V alloy manufactured by selective laser melting,” Materials Science and Engineering: A, vol. 802, Jan. 2021, doi: 10.1016/j.msea.2020.140649

[31] Shi, X., Yan, C., Feng, W., Zhang, Y., & Leng, Z. (2020). Effect of high layer thickness on surface quality and defect behavior of Ti-6Al-4V fabricated by selective laser melting. Optics and Laser Technology, 132. https://doi.org/10.1016/j.optlastec.2020.106471

[32] Promoppatum, P., Onler, R., & Yao, S. C., “Numerical and experimental investigations of micro and macro characteristics of direct metal laser sintered Ti-6Al-4V products”, Journal of Materials Processing Technology, 240, 262–273, 2017. Doi: 10.1016/j.jmatprotec.2016.10.005

[33] B. Song, S. Dong, B. Zhang, H. Liao, and C. Coddet, “Effects of processing parameters on microstructure and mechanical property of selective laser melted Ti6Al4V,” Mater Des, vol. 35, pp. 120–125, Mar. 2012, doi: 10.1016/j.matdes.2011.09.051.

TABLE 1. EFFECT OF PROCESS PARAMETERS ON THE TENSILE PROPERTIES OF TI-6AL-4V

Ref.	**System**	**Machine**	**Process parameters**					**Tensile properties**		
			Laser power (W)	***Scanning speed (mm/s)***	***Hatch spacing (mm)***	***Layer thickness (mm)***	***Energy density (J/mm^3)***	***Ultimate tensile strength (MPa)***	***Yield strength (MPa)***	***Elongation (%)***
10	SLM	Trumpf LF250	160	600	0.200	0.040	33	1206	1137	7.6
11	SLM	Realizer SLM 100	200	1000	0.100	0.050	40	1269	1195	5.0
12	SLM	SLM 250 HL	375	1029	0.120	0.060	51	1150	1106	11.4
13	SLM	EOS M 290	280	1200	0.140	0.030	56	1223.5	1128	9.7
14	L-PBF	The mLAB	65	520	0.077	0.025	65	1437	1250	5.6
15	L-PBF	Renishaw AM400	200	1500	0.065	0.030	68	1200	-	6.1
16	SLM	ENAVISION 250P	190	900	0.100	0.030	70	1161	-	-
17	SLM	RenAM250	200	900	0.105	0.030	71	1200	1150	6
6	SLM	EOS M270 DMLS	120	540	0.100	0.030	74	1257	1150	8.0
18	L-PBF	Trumpf Truprint 1000	90	905	0.060	0.020	83	1193	992.6	4.8
19	SLM	LM-Q	250	1600	0.060	0.030	87	1267	1110	7.3
20	SLM	Realizer SLM 150	110	500	0.050	0.050	90	1246	1150	5.0
21	SLM	EOS M290	280	1200	0.050	0.050	93	1241	1065	6.0
6	SLM	EOS M270 DMLS	120	400	0.100	0.030	100	1148	1066	5.4
22	SLM	MTT250	200	200	0.180	0.050	111	1035	910	3.3
23	SLM	SLM 250 Solution	175	600	0.100	0.025	117	1051	736	11.9
24	SLM	ProX DMP 320	79	620	0.082	0.030	127	1200	-	10.0
7	SLM	Self-developed SLM	194	1000	0.070	0.020	138	1268	1030	11.9
25	SLM	Concept laser M2	188	800	0.075	0.020	156	1200	1000	10.0
26	SLM	M3 linear	95	125	0.130	0.030	195	1250	1125	6.0
10	SLM	Trumpf LF250	160	600	0.200	0.040	33	1206	1137	7.6
11	SLM	Realizer SLM 100	200	1000	0.100	0.050	40	1269	1195	5.0

TABLE 2. EFFECT OF LASER POWER ON THE TENSILE PROPERTIES OF TI-6AL-4V

Ref.	System	Machine	Process parameters					Tensile properties		
			Laser power (W)	*Scanning speed (mm/s)*	*Hatch spacing (mm)*	*Layer thickness (mm)*	*Energy density (J/mm^3)*	*Ultimate tensile strength (MPa)*	*Yield strength (MPa)*	*Elongation (%)*
16	SLM	ENAVISION 250P	160	900	0.100	0.030	59.26	1053	-	-
			190				70.37	1126	-	-
			200				81.48	1139	-	-
24	SLM	3D Systems ProX DMP 320	70	620	0.082	0.030	113	1096.71	-	10.82
			79				127	1165.05	-	10.80
			88				142	1183.24	-	7.840
			97				156	1177.87	-	7.040
			106				171	1154.85	-	6.69
27	DMLS	EOSINT M280	150	1250	-	0.030	-	1145.60	-	25.86
			200					1386.10	-	23.80
			250					1438.50	-	27.36
			300					1656.70	-	35.74
28	SLM	3D Printing	300	-	-	-	-	1118.59	1017.55	6.11
			500					1277.71	1228.90	5.19
			800					1127.27	1048.66	4.76
29	L-PBF	RenAM 500M	100	-	0.100	0.030	-	388.87	264.81	0.62
			150					763.42	152.68	1.05
			200					959.05	959.05	1.92
			250					997.22	932.80	2.58
			300					1025.84	892.25	3.12
			350					994.83	901.79	3.52
			400					1020	931.53	3.03

TABLE 3. EFFECT OF SCANNING SPEED ON THE TENSILE PROPERTIES OF TI-6AL-4V

Ref.	System	Machine	Process parameters					Tensile properties		
			Laser power (W)	*Scanning speed (mm/s)*	*Hatch spacing (mm)*	*Layer thickness (mm)*	*Energy density (J/mm^3)*	*Ultimate tensile strength (MPa)*	*Yield strength (MPa)*	*Elongation (%)*
16	SLM	ENAVISION 250P	190	800	0.100	0.030	79.17	1140	-	-
				1000			63.33	1093	-	-
				1200			52.78	975	-	-
24	SLM	3D Systems ProX DMP 320	88	496	0.082	0.030	177	1196.20	-	5.80
				558			158	1196.20	-	6.63
				620			142	1193.25	-	6.96
				682			129	1190.30	-	9.62
				744			118	1175.53	-	10.20
27	DMLS	EOSINT M280	150	500	-	0.030	-	1145.60	-	25.86
				750				1176.70	-	26.80
				1000				1184.10	-	24.23
				1250				1245.40	-	30.62
28	SLM	3D Printing	500	4	-	-	-	1216.90	1096.71	2.01
				6				1096.71	1014.08	3.57
				8				826.29	698.59	3.83
				10				811.27	657.28	6.65
6	SLM	EOS M270 DMLS	120	960	0.100	0.030	42	1237	1098	8.8
				540			74	1257	1150	8.0
				400			100	1148	1066	5.4
				1260			32	1112	932	6.6
				1500			27	978	813	3.7
17	SLM	RenAM250	200	900	0.105	0.030	70.55	1200	1150	6
				1000			63.49	1140	1150	14-15

TABLE 4. EFFECT OF HATCH SPACING ON THE TENSILE PROPERTIES OF PBF TI-6AL-4V

Ref.	System	Machine	Process parameters					Tensile properties	
			Laser power (W)	*Scanning speed (mm/s)*	*Hatch spacing (mm)*	*Layer thickness (mm)*	*Energy density (J/mm^3)*	*Ultimate tensile strength (MPa)*	*Elongation (%)*
30	SLM	The Concept Laser M Lab R SLM device	100	1400	0.0225	0.025	126.98	863.47	3.72
					0.030		95.24	875.26	4.13
					0.0375		76.19	881.61	4.22
					0.045		63.49	916.97	4.35
					0.0525		54.42	975.00	4.46
					0.060		47.62	1033.03	4.23
					0.0675		42.33	1094.69	4.08
					0.075		38.095	1094.69	3.91
					0.0825		34.63	1061.14	3.83
					0.090		31.75	1054.79	3.56
					0.0975		29.30	1045.73	3.06
					0.105		27.21	1017.62	2.49
16	SLM	ENAVISION 250P	190	900	0.07	0.030	100.53	645	-
					0.09		78.19	1016	-
					0.11		63.97	991	-

TABLE 5. EFFECT OF LAYER THICKNESS ON THE TENSILE PROPERTIES OF TI-6AL-4V

Ref.	System	Machine	Ti-6Al-4V Size (µm)	Process parameters					Tensile properties		
				Laser power (W)	*Scanning speed (mm/s)*	*Hatch spacing (mm)*	*Layer thickness (mm)*	*Energy density (J/mm^3)*	*Ultimate tensile strength (MPa)*	*Yield strength (MPa)*	*Elongation (%)*
25	SLM	Concept laser M2	20-50	188	800	0.075	20	156	1200	1000	10.0
18	L-PBF	Trumpf Truprint 1000	10-50	90	905	0.060	20	83	1193	992.6	4.8
14	L-PBF	The mLAB	5-40	65	520	0.077	25	65	1437	1250	5.6
30	SLM	The M Lab R	~28	100	1400	0.0675	25	42	1094.7	-	4.08
23	SLM	SLM 250 Solution	31-53	175	600	0.100	25	117	1051	736	11.9
13	SLM	EOS M 290	20-53	280	1200	0.140	30	56	1223.5	1128	9.7
15	L-PBF	Renishaw AM400	15-45	200	1500	0.065	30	68	1200	-	6.1
16	SLM	ENAVISION 250P	~45	190	900	0.100	30	70	1161	-	-
19	SLM	LM-Q	-	250	1600	0.060	30	87	1267	1110	7.3
24	SLM	ProX DMP 320	6-47	79	620	0.082	30	127	1200	-	10.0
26	SLM	M3 linear	10-70	95	125	0.130	30	195	1250	1125	6.0
16	SLM	ENAVISION 250P	~45	190	900	0.09	30	78	1016	-	-
27	DMLS	EOSINT M280	4-40	150	1250	-	30	-	1245.4	-	30.6
29	L-PBF	RenAM 500M	20-100	300	-	0.100	30	-	1025.8	892.2	3.1
6	SLM	EOS M270 DMLS	~30	120	540	0.100	30	74	1257	1150	8.0
17	SLM	RenAM250	15-45	200	900	0.105	30	71	1200	1150	6
10	SLM	Trumpf LF250	20-55	160	600	0.200	40	33	1206	1137	7.6
11	SLM	Realizer SLM 100	~77	200	1000	0.100	50	40	1269	1195	5.0
20	SLM	Realizer SLM 150	45-75	110	500	0.050	50	90	1246	1150	5.0
21	SLM	EOS M290	10-70	280	1200	0.050	50	93	1241	1065	6.0
22	SLM	MTT250	~30	200	200	0.180	50	111	1035	910	3.3
12	SLM	SLM 250 HL	25-45	375	1029	0.120	60	51	1150	1106	11.4
31	SLM	Concept laser M2	18-106	400	140	0.100	100	286	1200	1100	10.2
31	SLM	Concept laser M2	18-106	400	60	0.100	200	333	1130	1040	7.57